Cell Reports
Article

A Function for EHD Family Proteins in Unidirectional Retrograde Dendritic Transport of BACE1 and Alzheimer's Disease Aβ Production

Virginie Buggia-Prévot,[1] Celia G. Fernandez,[2] Vinod Udayar,[4] Kulandaivelu S. Vetrivel,[1] Aureliane Elie,[1] Jelita Roseman,[1] Verena A. Sasse,[5] Margaret Lefkow,[2] Xavier Meckler,[1] Sohinee Bhattacharyya,[6] Manju George,[6] Satyabrata Kar,[5] Vytautas P. Bindokas,[3] Angèle T. Parent,[1] Lawrence Rajendran,[4] Hamid Band,[6] Robert Vassar,[7] and Gopal Thinakaran[1,2,*]

[1]Departments of Neurobiology, Neurology, and Pathology, The University of Chicago, Chicago, IL 60637, USA
[2]Committee on Neurobiology, The University of Chicago, Chicago, IL 60637, USA
[3]Department of Pharmacological and Physiological Sciences, The University of Chicago, Chicago, IL 60637, USA
[4]Systems and Cell Biology of Neurodegeneration, Division of Psychiatry Research, University of Zurich, 8008 Zurich, Switzerland
[5]Centre for Prions and Protein Folding Diseases, Departments of Medicine and Psychiatry, University of Alberta, Edmonton, AB T6G 2M8, Canada
[6]Eppley Institute for Research in Cancer and Allied Diseases and Fred & Pamela Buffett Cancer Center, University of Nebraska Medical Center, Omaha, NE 68198, USA
[7]Department of Cell and Molecular Biology, Feinberg School of Medicine, Northwestern University, Chicago, IL 60611, USA
*Correspondence: gopal@uchicago.edu
http://dx.doi.org/10.1016/j.celrep.2013.12.006

SUMMARY

Abnormal accumulation of β-secretase (BACE1) in dystrophic neurites and presynaptic β-amyloid (Aβ) production contribute to Alzheimer's disease pathogenesis. Little, however, is known about BACE1 sorting and dynamic transport in neurons. We investigated BACE1 trafficking in hippocampal neurons using live-cell imaging and selective labeling. We report that transport vesicles containing internalized BACE1 in dendrites undergo exclusive retrograde transport toward the soma, whereas they undergo bidirectional transport in axons. Unidirectional dendritic transport requires Eps15-homology-domain-containing (EHD) 1 and 3 protein function. Furthermore, loss of EHD function compromises dynamic axonal transport and overall BACE1 levels in axons. EHD1/3 colocalize with BACE1 and APP β-C-terminal fragments in hippocampal mossy fiber terminals, and their depletion in neurons significantly attenuates Aβ levels. These results demonstrate unidirectional endocytic transport of a dendritic cargo and reveal a role for EHD proteins in neuronal BACE1 transcytosis and Aβ production, processes that are highly relevant for Alzheimer's disease.

INTRODUCTION

Proteolytic processing of amyloid precursor protein (APP) by the transmembrane aspartyl protease β-site APP cleaving enzyme 1 (BACE1) initiates Aβ production, a key step in Alzheimer's disease pathogenesis (Vassar et al., 1999; Yan et al., 1999). It is extremely important to understand details of BACE1 trafficking and processing of APP in neurons because a single amino acid substitution adjacent to the BACE1 cleavage site of APP, which significantly reduces BACE1 cleavage and thus Aβ peptide generation in cultured cells, has been recently found to protect against disease onset as well as cognitive decline in the elderly without Alzheimer's disease (Jonsson et al., 2012). APP is a type I transmembrane protein that undergoes secretory and endocytic trafficking in neurons and is axonally transported (reviewed in Haass et al., 2012). Conversion of APP to Aβ requires coordination of its intracellular itinerary with that of its cleavage enzymes, which are also transmembrane proteins. In cultured cell lines and primary neurons, a subset of full-length APP is processed to generate Aβ. Extensive studies have used nonneuronal cells to identify the cellular organelles and sorting pathways involved in amyloidogenic processing of APP. Although a consensus has not yet emerged, there is a general agreement on the importance of endocytic trafficking of APP for Aβ production (reviewed in Thinakaran and Koo, 2008; Rajendran and Annaert, 2012; Haass et al., 2012). BACE1 activity is optimal at acidic pH in vitro (Vassar et al., 1999), lending further support to the notion that APP cleavage by BACE1 is initiated during transit in acidic endocytic compartments.

In nonneuronal cells, BACE1 cycles between plasma membrane and endosomes and shows predominant steady-state localization in endocytic organelles (Vassar et al., 1999; Huse et al., 2000; Chia et al., 2013). Two routes of BACE1 endocytosis, a clathrin and adaptor protein-2 complex (AP-2) dependent (clathrin-dependent) and an ADP-ribosylation factor 6 dependent (clathrin-independent), have been described (Prabhu et al., 2012; Sannerud et al., 2011; Das et al., 2013). A C-terminal

dual-function dileucine motif [^{495}DDISLL^{500}] appears to mediate both modes of BACE1 internalization (Prabhu et al., 2012; He et al., 2002). Although studies of BACE1 trafficking described above have been informative, most of these were conducted in nonneuronal cells. The sorting itinerary of transmembrane proteins can be fundamentally different in polarized neurons versus nonpolarized nonneuronal cells. Specifically, neuronal protein sorting involves specialized and intricate transport mechanisms such as transcytosis and activity-dependent endocytosis/recycling. Endosomal organelles are found distributed throughout the soma, dendrites, and axons (Lasiecka and Winckler, 2011). Neuronal endosomes traffic bidirectionally in axons and dendrites, adding to the complexity of the mechanisms that regulate endocytic transport in neurons. There is some indication in the literature that BACE1 localizes to dendrites and axons in neurons (Laird et al., 2005; Goldsbury et al., 2006; Zhao et al., 2007; Sannerud et al., 2011; Das et al., 2013). Compelling in vivo studies demonstrated that ~70% of Aβ released in the brain requires ongoing endocytosis and that synaptic activity regulates the vast majority of this endocytosis-dependent Aβ secretion (Cirrito et al., 2005, 2008). In agreement, APP and BACE1 get routed to acidic endocytic organelles in dendrites upon induction of neuronal activity (Das et al., 2013).

APP undergoes BACE1-mediated cleavage during anterograde axonal transport, and Aβ can be generated and released at or near presynaptic sites in vivo (Buxbaum et al., 1998; Lazarov et al., 2002; Sheng et al., 2002; Cirrito et al., 2005; Harris et al., 2010; Sokolow et al., 2012). Abnormal accumulation of BACE1 in axon terminals has been documented in Alzheimer's disease brain (Zhao et al., 2007). Nevertheless, the trafficking pathway(s) that account for dynamic sorting of BACE1 to axons has not been investigated in any detail. Here, we characterize the dynamics of endocytic BACE1 trafficking in hippocampal neurons and report that BACE1 internalized in dendrites is exclusively transported toward the soma, and this polarized transport requires the function of Eps15 homology domain-containing (EHD) 1 and EHD3 recycling regulatory proteins. Axonal sorting and dynamic axonal transport of BACE1 are impaired in neurons when EHD function is compromised. EHD1/3 colocalize with BACE1 and APP β-C-terminal fragments in vivo, and loss of EHD1 or 3 expression leads to diminution of Aβ production in hippocampal neurons. Together, these findings characterize unidirectional endocytic BACE1 transport in neurons and identify a role for EHD family proteins in neuronal BACE1 trafficking and Aβ production.

RESULTS

Selective Labeling of Internalized BACE1

In order to selectively visualize endocytosed BACE1, we designed a construct, termed BBS-BACE1-YFP, by introducing a 13-residue α-*b*ungarotoxin *b*inding site (BBS) near the N terminus of BACE1 (Figure S1A). BBS-tagged receptors have been shown to bind fluorescently labeled α-bungarotoxin (BTX) in live transfected cells (Sekine-Aizawa and Huganir, 2004). Addition of the BBS site did not affect the ability of BACE1 to process APP (Figure S1B). Transfected HeLa or HEK293 cells were allowed to internalize Alexa-Fluor (AF)-coupled BTX for 60 min at 37°C, at which point they were subjected to a brief acid wash to remove surface-bound BTX (Figure 1A). This strategy selectively labeled cells expressing BBS-BACE1-YFP, and there was a strong correlation (R^2 = 0.85; Pearson's r = 0.92; $p < 0.0001$) between BTX labeling and YFP fluorescence intensity (Figures 1B and 1C). In stably transfected HEK293 cells, BTX uptake increased with time over a 3 hr period (Figure 1D). In cells where only surface BACE1 was labeled with BTX at 12°C, acid wash quantitatively removed BTX binding (Figure S1C). We then performed the BTX uptake assay in transfected hippocampal neurons and imaged them after the acid wash. BTX labeling was evident in neurons transfected with BBS-BACE1-YFP, whereas it was virtually absent in untransfected neurons under the conditions employed in our study (Figure 1E). In neurons transfected with BBS-BACE1$_{LL/AA}$-YFP, a mutant that predominantly accumulates at the cell surface (Huse et al., 2000; Prabhu et al., 2012), even a brief, 2 min acid wash was sufficient to strip nearly all BTX labeling (Figure S1D). Thus, the BTX uptake assay allows us to selectively visualize endocytosed BACE1 in transfected neurons.

Internalized BACE1 Undergoes Exclusive Retrograde Transport in Dendrites

In normal human brain, BACE1 localizes to the neuronal soma, dendrites, and axons; BACE1 distribution overlaps with that of MAP2 in apical dendrites of hippocampal neurons (Figure S2A). In cultured hippocampal neurons (12 days in vitro; DIV12), BACE1-YFP localized to both the somatodendritic compartments and the axons (Figures S2B and S2C). In dendrites, BACE1 can be found along the dendritic surface and in internal carriers as well as within dendritic spines, which are closely apposed to presynaptic sites marked by Bassoon immunostaining (Figures S2C and S2D). Endocytosed BACE1 also localized to both somatodendritic compartments and axons of hippocampal neurons, as determined by MAP2 immunostaining following BTX uptake (Figure 2A). In order to visualize the dynamic transport of total BACE1 (YFP fluorescence) or internalized BACE1 (BTX fluorescence) in dendrites, we performed live-cell imaging. There was substantial variability in BACE1 motility in different dendritic branches of each neuron during the period of image acquisition, such that vesicles containing BACE1 underwent active transport in some dendrites, whereas they remained largely stationary in others. Therefore, we focused on dendrites that exhibited the greatest BACE1 vesicle motility in each neuron and generated kymographs to analyze the results (Figures 2B and 2C; Movies S1 and S2). As expected, BACE1-YFP fluorescence was observed in vesicles that were transported in both anterograde and retrograde directions along dendrites. Quantitative analysis revealed that an approximately equal number of BACE1-containing vesicles underwent anterograde and retrograde transport (Figure 2C). Intriguingly, we found that nearly all of the motile vesicles (>95%) containing internalized BACE1 underwent retrograde transport, toward the cell body in proximal (Figures 2B and 2C; Movie S1) as well as in distal dendritic segments (Figure 2D; Movie S2). This vectorial retrograde movement of BTX-labeled endocytic BACE1 in dendrites was unexpected because, to our knowledge, this has not previously

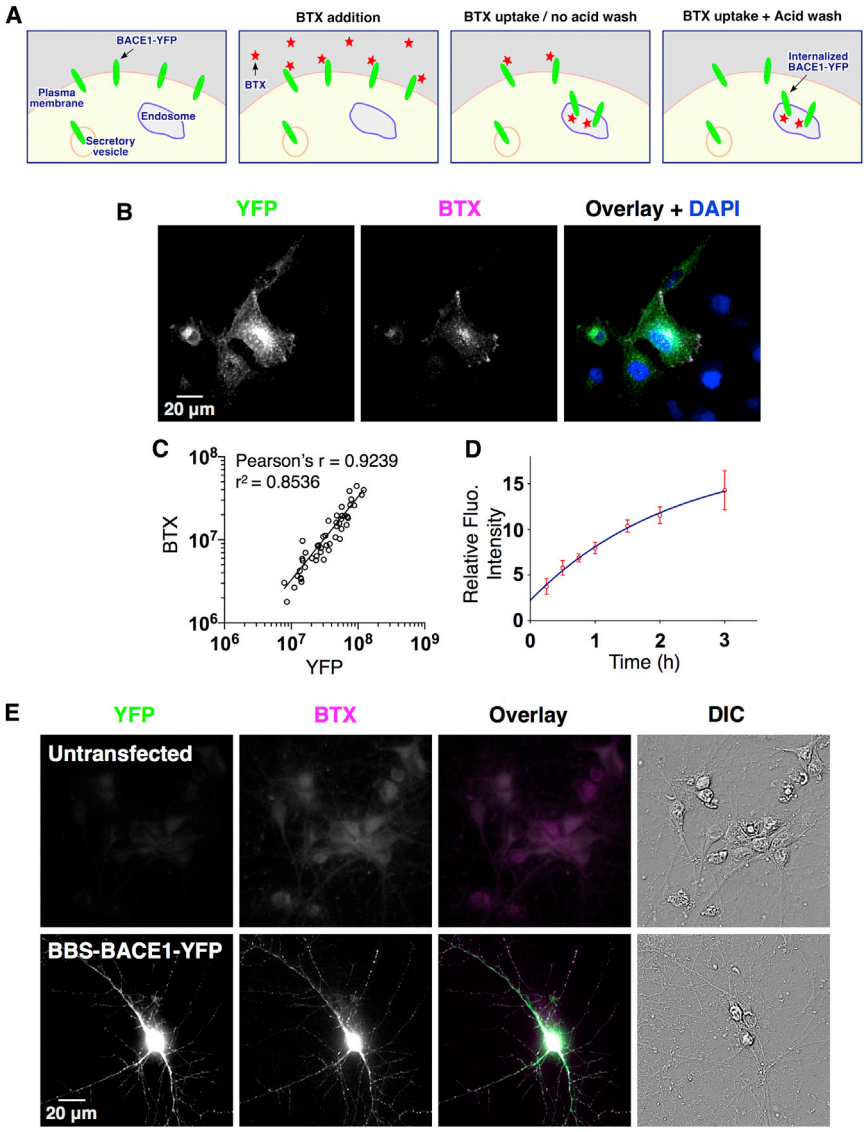

Figure 1. BTX-Labeling Strategy to Selectively Visualize Internalized BACE1

(A) The schematics of the assay used to label internalized BACE1 using fluorescently tagged BTX.

(B and C) Development of the BTX-labeling assay. HeLa cells grown on coverslips were transiently transfected with BBS-BACE1-YFP and incubated with AF555-BTX at 37°C for 1 hr. The coverslips were washed with ice-cold HBSS and subjected to an acid wash to remove surface-bound BTX before fixing. YFP and BTX fluorescence intensities were quantified from individual cells and plotted (n = 50 cells).

(D) HEK293 cells stably expressing BBS-BACE1-YFP were cultured in 96-well dishes and incubated with AF647-BTX for different periods of time. The cells were subjected to an acid wash before fixing. AF647-BTX fluorescence intensity was quantified using a Tecan Safire2 microplate reader and converted to fold differences using an intensity standard generated by different cell-plating densities. n = 3 independent experiments, each performed in triplicates.

(E) BTX labeling of internalized BACE1 in hippocampal neurons. DIV12 neurons transfected or not with BBS-BACE1-YFP were incubated with AF647-BTX for 4 hr at 37°C. The coverslips were subjected to acid wash before fixing. z stacks were acquired and projected onto a single plane to visualize YFP and BTX fluorescence. Identical conditions were used for image acquisition and processing for untransfected and BBS-BACE-YFP-transfected cells.

See also Figure S1.

been observed by live-cell imaging for any transmembrane protein in dendrites. This exciting finding demonstrates that following internalization from the dendritic cell-surface, BACE1 undergoes vectorial transport toward the soma for further sorting or degradation. In contrast to unidirectional dendritic transport, BTX-labeled internalized BACE1 underwent both anterograde and retrograde transport in axons, in a manner similar to total BACE1 (Figure 2E; Movie S3).

We used endogenous organelle markers to characterize the distribution of endocytic BACE1 in dendrites of hippocampal neurons. Confocal microscopy analysis showed that both total BACE1 and internalized BACE1 localized to early endosomes (marked by NEEP21 or EEA1). The extent of colocalization was quantified using Manders' coefficient (Figures 3A and S3). Recycling endosome localization (marked by transferrin receptor [TfR]) of internalized BACE1 was also apparent in dendrites (Figures 3A, 3B, and S3). We confirmed recycling endosome localization of internalized BACE1 using Rab11b, a GTPase well characterized for regulating slow recycling of many endocytic cargos, including TfR (Sönnichsen et al., 2000). We cotransfected neurons with BACE1-YFP and a mCherry-tagged Rab11B construct similar to one previously employed to characterize recycling endosome membrane domains (Sönnichsen et al., 2000). We found that internalized BTX-labeled BACE1 colocalized with mCherry-Rab11B in dendrites and axons (Manders' coefficient 0.66 ± 0.09 and 0.28 ± 0.15, respectively) (Figure 3D).

EHD Proteins Colocalize with BACE1 and APP β-CTFs In Vivo, and Their Depletion in Hippocampal Neurons Decreases Aβ Levels

Members of the EHD protein family function in membrane tubulation and vesicle fission processes and are thought to coordinate Rab GTPase-mediated endocytic vesicular trafficking of early as well as recycling endosomes in nonneuronal cells and neurons (Lasiecka et al., 2010; Naslavsky and Caplan, 2011; Lasiecka and Winckler, 2011). Because endogenous EHD proteins could not be reliably detected in cultured hippocampal neurons using currently available antibodies, we utilized

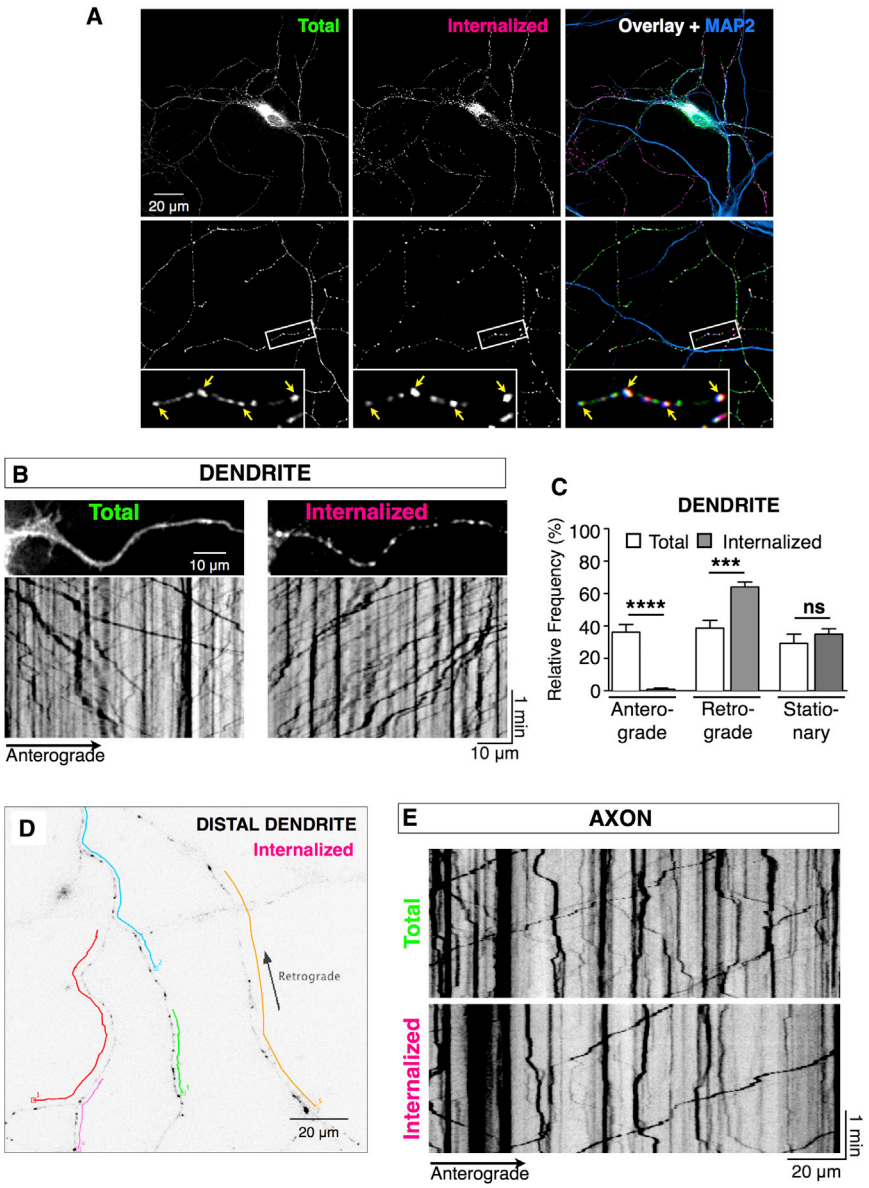

Figure 2. Dynamic Characteristics of Internalized BACE1

(A) Localization of internalized BACE1 in dendrites and axons. DIV12 neurons were transfected with BBS-BACE1-YFP and internalized BACE1 was labeled by incubation with AF647-BTX for 4 hr at 37°C followed by acid wash to remove surface-bound BTX. Deconvolved images of a transfected neuron depict the distribution of total and internalized pool of BACE1 in the cell body and dendrites (top) and the corresponding axonal network (bottom).

(B) Unidirectional transport of internalized BACE1 in dendrites. Time-lapse images of total (YFP fluorescence) and internalized BACE1 (BTX fluorescence) were sequentially acquired following AF647-BTX uptake, at the rate of one frame/sec for 3 min. Images of a dendritic segment, with the cell body on the left, and the corresponding kymographs of total and internalized BACE1, are shown.

(C) Quantification of total and internalized BACE1 motility in dendrites (n = 760 total and 699 internalized carriers from 18 neurons). Error bars represent SEM. Unlike the bidirectional transport of total BACE1 in dendrites, internalized BACE1 undergoes transport exclusively in the retrograde direction.

(D) A still image from the first frame of Movie S2 depicting internalized BACE1 dynamic transport in a distal dendrite. The retrograde transport tracks of representative transport vesicles in different branches of the same dendrite are indicated.

(E) Dynamic axonal transport of internalized BACE1. Time-lapse images of total and internalized BACE1 were sequentially acquired from neurons following AF555-BTX uptake, at the rate of one frame/sec for 3 min. Bidirectional axonal transport of total and internalized BACE1 were visualized by generating kymographs.

See also Figure S2.

previously described DsRed-tagged EHDs (George et al., 2007). In transfected neurons, EHD1 and EHD3 colocalized with BACE1 in dendrites, dendritic spines, and neuronal soma, as well as in axons (Figures 4A–4C). Internalized BACE1, labeled using BTX uptake, also showed extensive colocalization with EHD1 and EHD3 in dendrites and dendritic spines, and along the axons (Figures 4A and 4B). Results of Manders' coefficient of colocalization are depicted in (Figure 4C). Together, the results described above show that a significant fraction of BACE1 localizes to endocytic organelles along dendrites and axons.

Three of the four known mammalian EHD proteins (EHD1, EHD3, and EHD4) were detected in mouse brain lysates by immunoblot analysis (George et al., 2007), but the cellular and subcellular localization of EHDs in the brain is unknown. To determine whether EHD proteins are expressed in the hippocampus, we immunostained mouse brain sections using antibodies that specifically recognize individual EHD family members (George et al., 2007) and performed confocal microscopy analysis. Consistent with the immunoblot data, expression of EHD1, EHD3, and EHD4 was readily detectible by immunostaining in mouse brain, whereas EHD2 was not detectable (Figures 5 and S3). Interestingly, EHD1 and EHD3 prominently localized in hippocampal mossy fibers where they colocalized with BACE1 (Figure 5A). EHD4 expression was mainly restricted to the cell bodies of neurons in the dentate gyrus and CA1–CA3 (Figure S4).

To assess whether EHD1 and 3 function in endosomal trafficking affects amyloidogenic processing of APP, we analyzed the effect of small interfering RNA (siRNA) knockdown of EHD1 and EHD3 in cultured neurons. In these experiments, we achieved knockdown efficiencies of 64% (EHD1) and 61% (EHD3) 72 hr after transfection with siRNAs, as assayed by quantitative PCR. Media conditioned by siRNA-treated neurons were

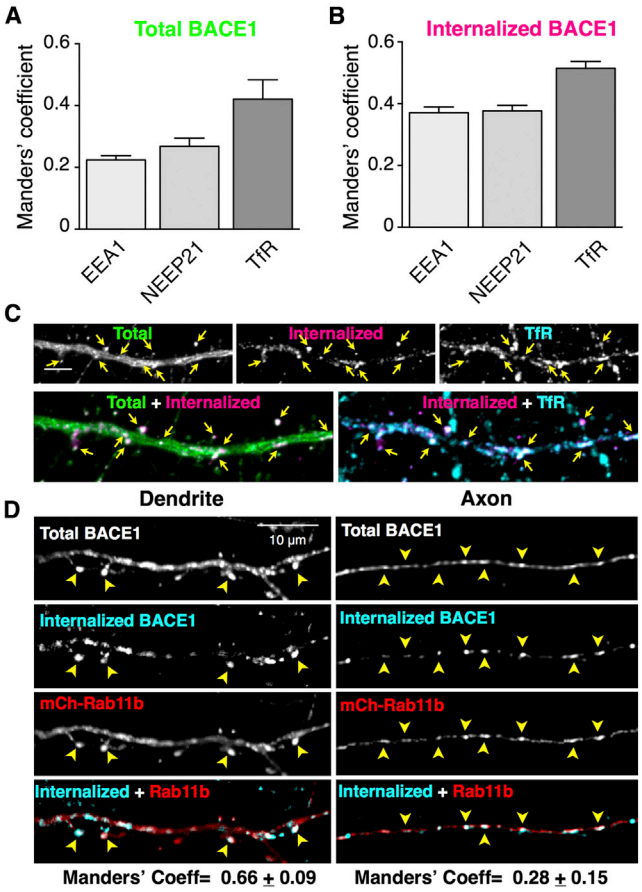

Figure 3. Subcellular Localization of Internalized BACE1

(A and B) Neurons transfected with BBS-BACE1-YFP were labeled by AF647-BTX uptake, subjected to acid wash, and immunolabeled for EEA1, NEEP21, and TfR. Manders' coefficient of colocalization with endosome markers was quantified by confocal microscopy for total BACE1 [YFP] (A; n = 11–16 neurons) and internalized BACE1 [BTX fluorescence] (B; n = 7–13 neurons). Representative confocal images are depicted in Figure S3.

(C) Representative confocal images of a dendrite segment depicting colocalization of internalized BACE1 dendrites and spines with endogenous TfR. Scale bar, 10 μm.

(D) Neurons cotransfected with BACE1-YFP and mCherry-Rab11b were labeled by AF647-BTX uptake, subjected to acid wash, and immunostained for MAP2. The extent of colocalization of Rab11b and internalized BACE1 in dendrites and axons was quantified (n = 8 neurons).

Error bars represent SEM. See also Figure S3.

assayed using a sensitive electrochemiluminescence assay to quantify the levels of secreted Aβ. We observed a significant decrease of Aβ38, Aβ40, and Aβ42 peptides secreted by neurons following knockdown of EHD1 or EHD3 (Figure 4D).

To determine whether EHD's influence on APP processing might be relevant in vivo, we examined colocalization between EHD and BACE1-cleaved APP β-C-terminal fragments (β-CTF) in a transgenic mouse model of Alzheimer's disease pathogenesis. Confocal analysis revealed that both EHD1 and EHD3 show substantial overlap with APP β-CTF and/or Aβ in mossy fiber terminals in APPswe/PS1ΔE9 transgenic mouse brain (analyzed at 2 months, before the onset of overt extracellular Aβ deposition) (Figure 5B), suggesting that in mouse brain, BACE1 in EHD-positive structures likely mediates the processing of APP to β-CTF, the precursor of Aβ. Together, these results suggest a role for EHD1 and EHD3 in APP processing in neurons.

EHD1 and EHD3 Regulate Dynamic BACE1 Transport in Hippocampal Neurons

The results described above prompted us to investigate whether EHD1 and EHD3 coordinate BACE1 transport in neurons. For these studies, we chose to employ a dominant-negative (DN) approach that has been successfully used in previous investigations (George et al., 2007; Yap et al., 2010) because DN plasmids can be efficiently transfected into mature neurons to compromise EHD function in less than 24 hr (unlike siRNA approach, which requires 3 days to achieve knockdown of EHD expression following transfection of young neurons at DIV5). We performed live-cell imaging and generated kymographs to assess whether unidirectional retrograde transport of internalized BACE1 was affected by expression of EHD DN mutants that lack the EH domain (EHD-ΔEH) (Figure 6A; Movie S4). Quantitative analysis revealed a significant decrease in the fraction of retrograde transport of dendritic carriers containing internalized BACE1 in neurons expressing DN mutant EHD1 or EHD3 as compared with those expressing wild-type (WT) proteins (Figure 6B). This effect was extremely robust such that a marked reduction in retrograde transport of vesicles was evident just from quantification of total BACE1 transport in dendrites; nevertheless, anterograde transport of BACE1-YFP remained unchanged by DN EHD expression (Figure 6B). Together, these results reveal a functional requirement of EHD1 and EHD3 for the dynamic retrograde transport of BACE1-containing endosomes in dendrites.

We then asked whether EHD function was required for membrane sorting of internalized BACE1 in endocytic organelles and/or for the retrograde transport of BACE1 in endocytic carriers. Coexpression of EHD1-ΔEH or EHD3-ΔEH with BACE1 had no significant effect on steady-state BACE1 localization at the dendritic surface, as measured by surface BTX labeling (the surface/total fluorescence ratios normalized to vector controls were EHD1 WT, 1.0 ± 0.11; EHD1-ΔEH, 0.89 ± 0.12; EHD3 WT, 1.0 ± 0.21; EHD3-ΔEH, 1.05 ± 0.13 [p = 0.9272; n = 21–28 neurons each]). In agreement, localization of endocytosed BACE1 in somatodendritic compartments following BTX uptake was apparent in neurons transfected with WT or DN EHDs (Figure 7A). Quantitative analysis of organelle marker staining revealed no increase of internalized BACE1 in endosomes positive for EEA1 or NEEP21, suggesting that that the expression of EHD-ΔEH mutants did not cause a retention of internalized BACE1 in early endosomes (Figure S5). Furthermore, there was no decrease in the extent of colocalization with TfR, suggesting that internalized BACE1 is able to reach TfR-positive recycling endosomes (Figure S5). We noted a small increase in the extent of BACE1 colocalization with TfR in neurons expressing DN EHD proteins. This increase may be mechanistically important because EHD1/3 could regulate BACE1 exit from the TfR-positive endocytic recycling compartment.

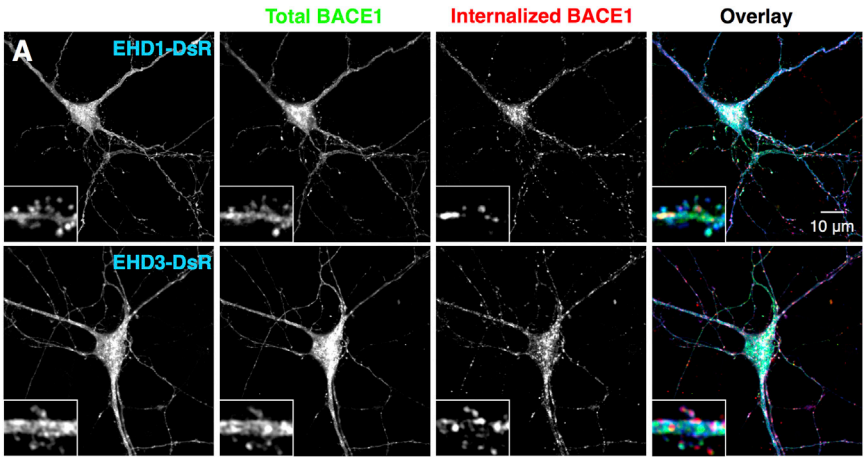

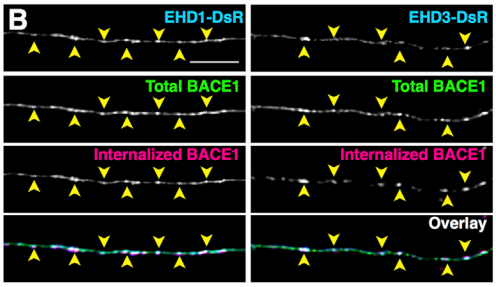

C

		EHD1	EHD3
Dendrites	Total BACE1	0.594 +/- 0.09	0.569 +/- 0.08
	Internalized BACE1	0.588 +/- 0.09	0.577 +/- 0.1
Axons	Total BACE1	0.620 +/- 0.17	0.477 +/- 0.10
	Internalized BACE1	0.471 +/- 0.2	0.467 +/- 0.14

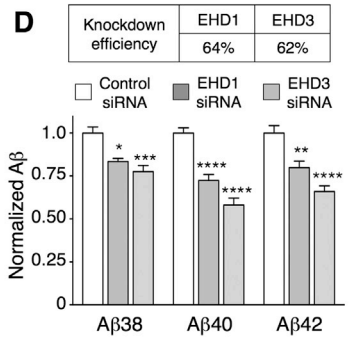

Figure 4. Colocalization of Internalized BACE1 with EHD1 and EHD3 and Neuronal Aβ Production following EHD Knockdown

(A) Neurons cotransfected with BBS-BACE1-YFP and DsRed-tagged EHD1 or EHD3 were labeled by AF647-BTX uptake, subjected to acid wash, and analyzed by confocal microscopy. Insets show magnified segments of dendrites.

(B) Images of representative axon segments show colocalization of internalized BACE1 with EHD1 and EHD3 in tubulovesicular carriers.

(C) Manders' coefficient of colocalization of total or internalized BACE1 with EHD1 (n = 16 neurons) or EHD3 (n = 12 neurons) was quantified.

(D) Primary neurons were transfected with siRNA against EHD1 or EHD3. A scrambled siRNA was used as the negative control. The levels of Aβ38, Aβ40, and Aβ42 in the conditioned media were quantified by ELISA and normalized to control siRNA (n = 4 technical replicates).

Error bars represent SEM.

In neurons expressing DN EHD1/3, we observed a diminution of BACE1 levels in axons. We carefully quantified the fluorescence intensities along dendrites and axon segments in individual neurons following BTX uptake. The results show a significant decrease in the mean fluorescence intensity in axons versus dendrites (axon/dendrite ratio) of total BACE1 as well as internalized BACE1 in neurons expressing EHD-ΔEH mutants as compared with WT EHDs or empty vector control (Figure 7B). The diminution of total BACE1 levels in axons in addition to internalized BACE1 suggest that this decrease is not simply due to defects in local axonal recycling of BACE1. Finally, we sought to determine if this decrease is due to a loss of a dynamically transported pool of BACE1 in axons. Indeed, live-cell imaging of neurons transfected with EHD1 or EHD3 DN mutants revealed a significant decrease in the number of motile BACE1-YFP-containing carriers in axons (Figures 7C and 7D; Movie S5). Although the effect on BACE1 axonal transport is quite striking, live-cell imaging of neurons cotransfected with NPY-mCherry revealed apparently unperturbed dynamic bidirectional transport of trans-Golgi-network (TGN)-derived vesicles in neurons expressing EHD-ΔEH mutants (Figure 7E). Thus, EHD1 and EHD3 function is required for efficient sorting of BACE1 to axons (as evidenced by a decrease in axon:dendrite ratio) as well as dynamic axonal transport of BACE1-containing vesicles.

DISCUSSION

Our study reveals a mode of vesicular trafficking in neurons, specifically, unidirectional retrograde transport of internalized cargo in dendrites. We demonstrate exclusive dendritic retrograde transport of internalized BACE1 in hippocampal neurons. Furthermore, our results show that somatodendritic and axonal BACE1 distribution in neurons is dynamically modulated by endocytic sorting in a trafficking pathway that requires EHD protein function. Endogenous EHD proteins colocalize with BACE1 in hippocampal mossy fibers, and loss of EHD1 or EHD3 expression in cultured neurons results in a significant decrease of Aβ secretion. These findings on EHD regulation of BACE1 trafficking and axonal targeting and Aβ production in neurons provide insights into presynaptic Aβ release and are highly relevant to abnormal presynaptic accumulation of BACE1 near amyloid plaques documented in Alzheimer's disease.

Dynamic Transport of BACE1 in Hippocampal Neurons

With a few exceptions, investigations on BACE1 trafficking have relied on nonpolarized cells to define intracellular sorting of BACE1 between plasma membrane, endosomes, the TGN, and lysosomes. The results of our live-cell imaging studies in hippocampal neurons provide information on polarized transport of BACE1 and implicate EHD proteins in endocytic sorting and axonal transport of BACE1. Although analysis of total BACE1-YFP fluorescence revealed bidirectional transport in dendrites with no obvious bias in directionality, a clear bias in retrograde transport toward the soma was observed in dendrites when the internalized BACE1 pool was selectively visualized. Internalized BACE1 either remained stationary or underwent exclusive retrograde transport toward the soma (Figure 2; Movies S1 and S2). On the other hand, total BACE1 and internalized BACE1

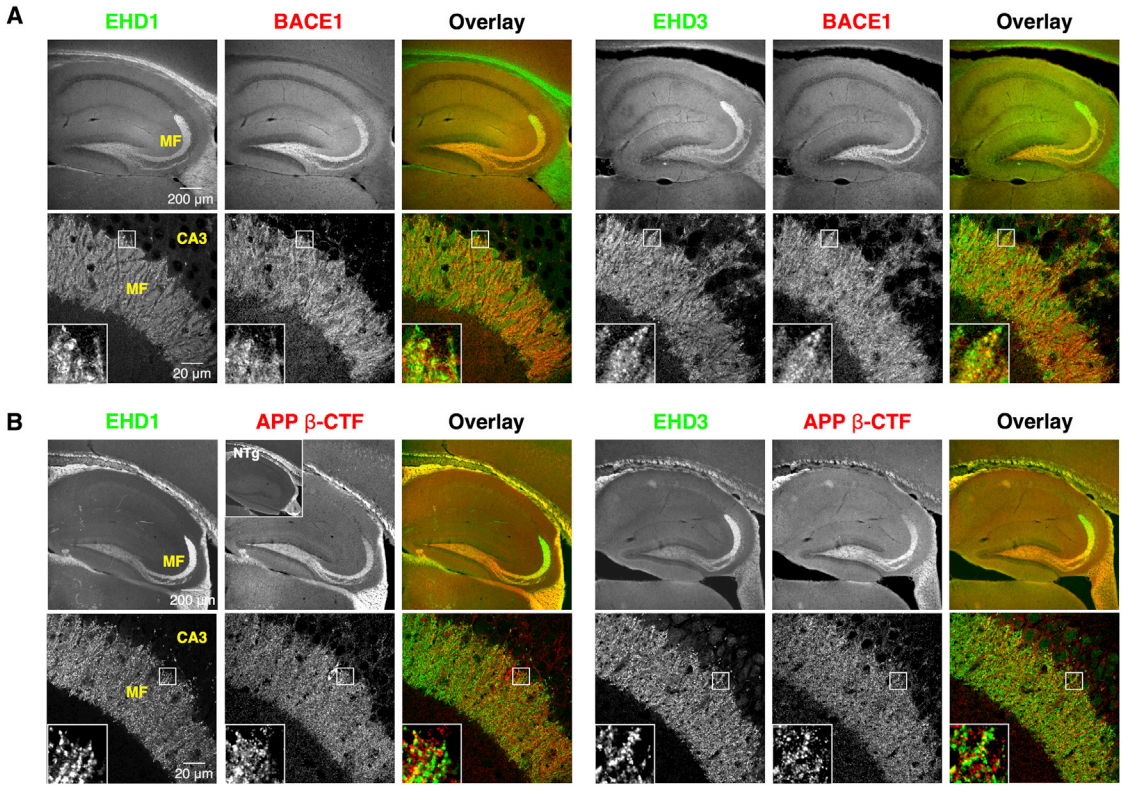

Figure 5. Colocalization of Endogenous EHD1 and EHD3 with BACE1 and APP β-CTFs in Mouse Brain

(A) Sagittal sections of P19 mouse brain were immunostained with antibodies against BACE1 and EHD1 or EHD3 and confocal images were acquired using 10× (top) and 100× objectives (bottom). Insets show higher magnification of the boxed area within the terminal field of mossy fibers (MF).

(B) Sagittal sections of 2-month-old APP/PS1 transgenic mouse brain were stained with antibodies against APP β-CTF (monoclonal antibody [mAb] 3D6) and EHD1 or EHD3 and analyzed by confocal microscopy. Lack of strong mAb 3D6 staining in mossy fibers of nontransgenic mice (NTg, inset) indicates the selectively of this antibody for APP β-CTFs and/or Aβ.

See also Figure S4.

underwent bidirectional axonal transport. The vectorial transport of internalized BACE1 in dendrites shares some similarity with the overall fate of receptors such as L1/NgCAM and TrkA, which are axonally targeted following endocytosis from the somatodendritic cell surface (Yap and Winckler, 2012). However, our live-cell imaging results of BACE1 endocytic transport characterize the dynamic and exclusive retrograde transport of endocytosed transmembrane protein cargo from dendrites.

The bidirectional and saltatory nature of BACE1 transport in neurons are characteristics of microtubule-based transport. Unlike the uniform orientation of microtubules in axons with their plus ends distal to the cell body, dendrites of mature neurons have an equal number of microtubules with their plus ends oriented toward or away from the cell body (Baas et al., 1988). Therefore, it is remarkable that dynamic transport of internalized BACE1 is bidirectional in axons, whereas it is only retrograde in dendrites. Not only do the transport vesicles containing internalized BACE1 need to distinguish between the plus end and minus end of microtubules in the near vicinity, they must also employ long-range guidance cues in order to navigate through dendritic branch points in a unidirectional manner and progressively move toward the soma (see Movie S2). In comparison, TfR and internalized transferrin are known to undergo bidirectional transport in dendrites (Prekeris et al., 1999; Burack et al., 2000; Lasiecka et al., 2010; Farías et al., 2012; data not shown). How internalized BACE1-containing endosomes in dendrites achieve unidirectional retrograde movement toward the soma, despite microtubule orientation in both directions, is an intriguing question that will require further studies.

EHD Proteins Function in Transport of Internalized BACE1

The four mammalian EHD paralogs show partial overlap in intracellular localization and function as homo- or hetero-oligomers. Together, they regulate endocytic trafficking of a number of receptors such as TfR, GLUT4 glucose transporter, AMPA receptor, and L1/NgCAM (Naslavsky and Caplan, 2011). We found that, in mouse brain, EHD1 and EHD3 colocalized with BACE1 and APP β-C-terminal fragments in large mossy fiber terminals. In cultured hippocampal neurons, expression of EHD1-ΔEH or EHD3-ΔEH DN mutant resulted in the loss of retrograde transport of internalized BACE1 in dendrites. However, because EHD DN expression did not cause aberrant retention of internalized BACE1 in EEA1- or NEEP21-positive early

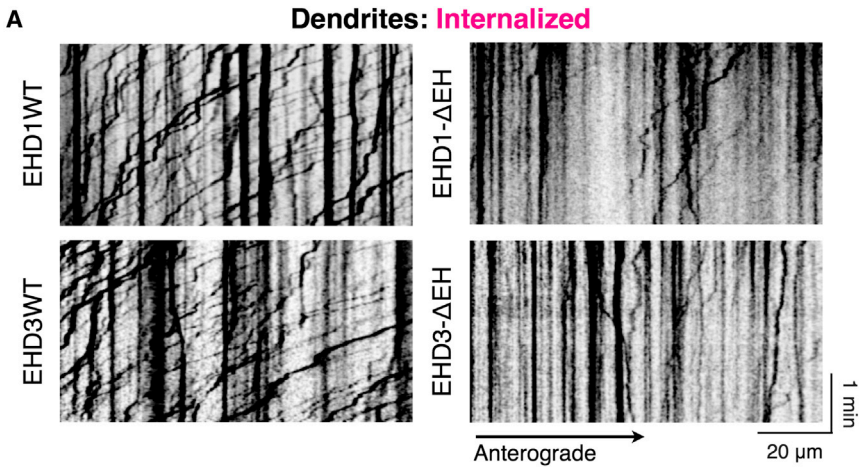

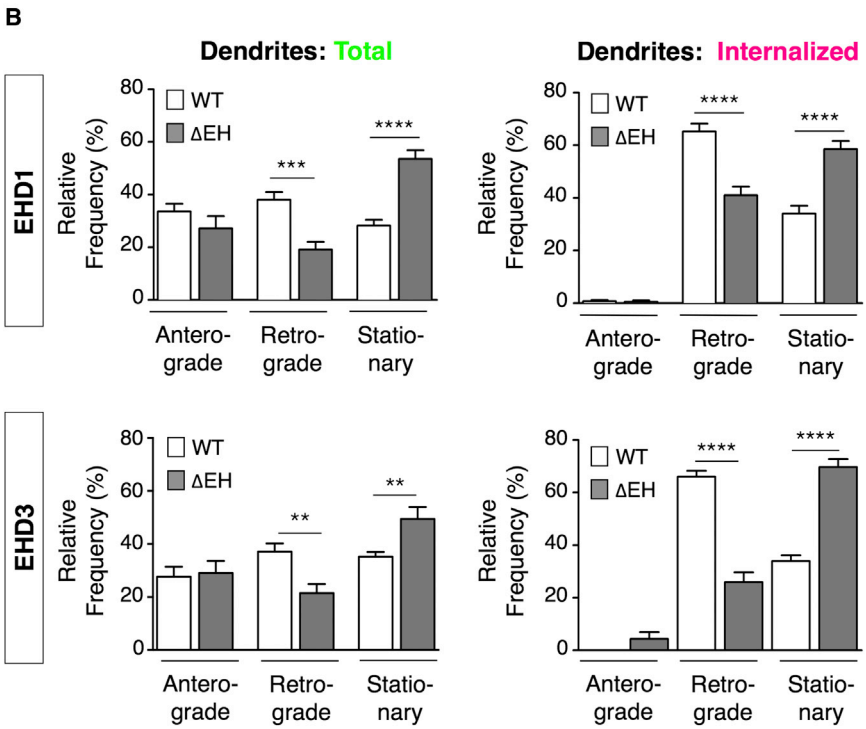

Figure 6. EHD1 and EHD3 Are Required for Retrograde Transport of Internalized BACE1 in Dendrites

(A) Neurons cotransfected with BBS-BACE1-YFP and the indicated DsRed-tagged EHD WT or EHD-ΔEH construct were labeled by AF647-BTX uptake. Representative kymographs of internalized BACE1 transport in dendrites are shown.

(B) Quantification of total and internalized BACE1 motility in dendrites. EHD1 WT n = 679 total (T) and 312 internalized (I) vesicles from 13 neurons; EHD1-ΔEH n = 427 T- and 227 I-vesicles from eight neurons; EHD3 WT n = 546 T and 291 I-vesicles from 12 neurons; EHD3-ΔEH n = 462 T- and 182 I-vesicles from nine neurons.

Error bars represent SEM.

endosomes, it appears that the initial steps in membrane sorting of BACE1 upon endocytosis in dendrites are EHD independent. In axons, there was an overall decrease in the levels of total as well as internalized BACE1 (Figures 7A and 7B). Interestingly, the loss of the motile BACE1 pool in axons is particularly striking, especially when transport of TGN-derived vesicles was unperturbed by DN EHD expression (Figures 7C and 7E). Together, these findings indicate that EHD1 and EHD3 have a critical role in endosomal transport of BACE1 and axonal targeting and/or sorting of motile vesicles containing BACE1. It is known that endosomes containing EHD1 traffic bidirectionally along dendrites (Lasiecka et al., 2010). Internalized BACE1 shows clear colocalization with EHD1 and EHD3 (Figure 4). Yet, nearly all the motile vesicles containing internalized BACE1 in dendrites undergo retrograde transport toward the soma, raising the possibility that BACE1 might play an active role in vectorial transport of a subset of endocytic vesicles in hippocampal neurons.

Endocytic Transport of BACE1 Is Distinct from Transcytosis of Cell Adhesion Molecules

The characteristics of endocytic sorting and the ultimate fate of internalized BACE1 in hippocampal neurons share some similarities, but also differ considerably, when compared with trafficking of cell adhesion molecules such as Caspr2 and L1/NgCAM, which also undergo endocytic sorting following internalization from the somatodendritic compartment. Unlike Caspr2 or L1/NgCAM, BACE1 is uniformly distributed on the surface of dendrites and axons at steady state, and internalized BACE1 is also readily detected in both dendrites and axons. Overexpression of either WT or DN EHD proteins markedly reduces L1/NgCAM endocytosis in dendrites (Yap et al., 2010). However, this does not appear to be the case for BACE1; colocalization of internalized BACE1 with EEA1, NEEP21, and TfR was not reduced by EHD DN expression. Instead, retrograde motility of internalized BACE1-containing vesicles in dendrites was compromised. In the case of Caspr2, nonpolarized biosynthetic delivery to somatodendritic and axonal plasma membrane is followed by compartment-specific endocytosis and elimination of somatodendritic Caspr2 (Bel et al., 2009). By contrast, biosynthetic L1/NgCAM internalized from the somatodendritic plasma membrane is transported in nondegradative endosomes and delivered to axonal plasma membrane (Yap et al., 2008). Similar to L1/NgCAM, endocytic elimination does not appear to be the reason why BACE1 internalized from dendrites is transported to the soma. Rather, loss of retrograde transport in dendrites is

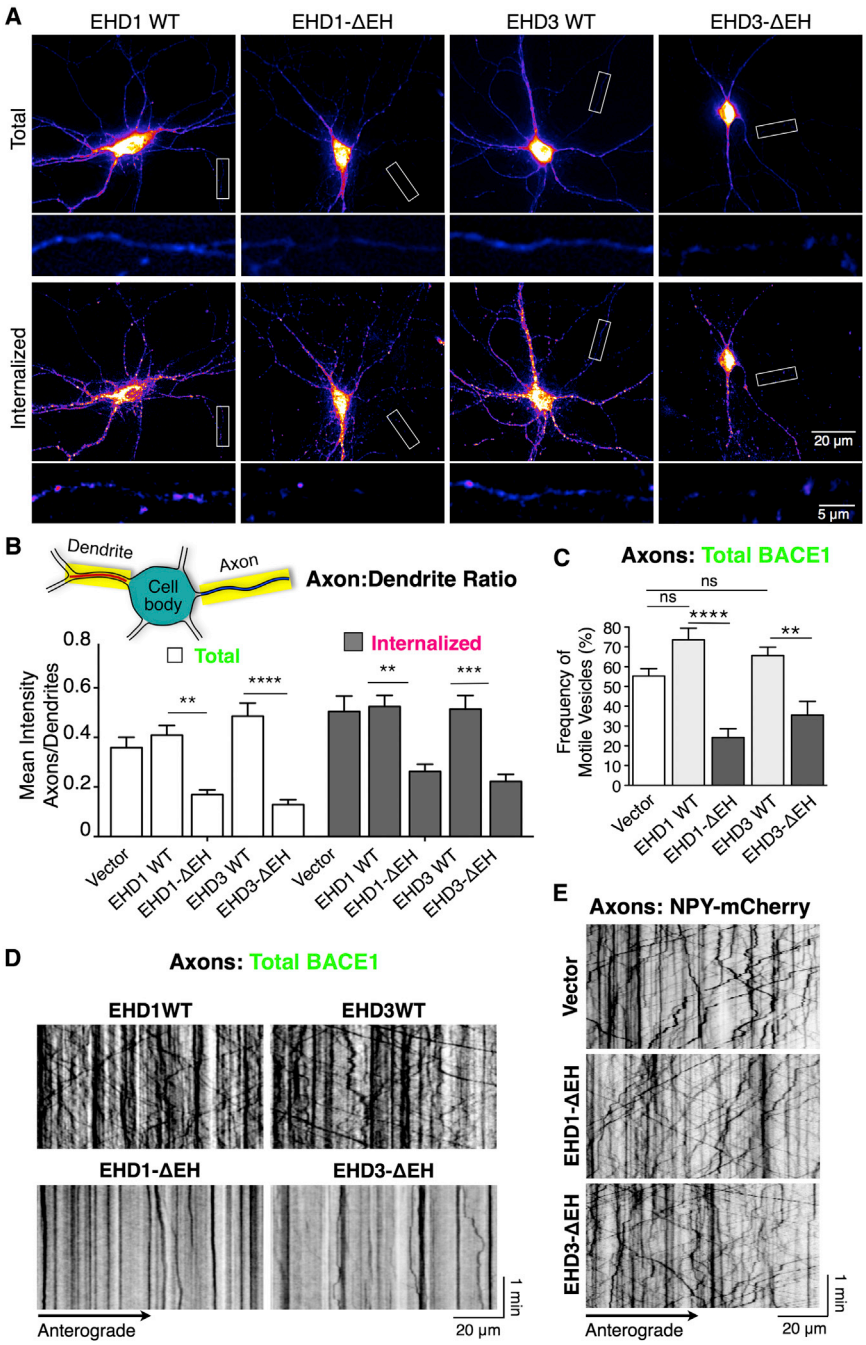

Figure 7. EHD1 and EHD3 Are Required for Axonal Localization and Dynamic Axonal Transport of BACE1

(A) Neurons were cotransfected with BBS-BACE1-YFP, and the indicated DsRed-tagged EHD WT or EHD-ΔEH construct were labeled by AF647-BTX uptake, subjected to acid wash, and immunostained for MAP2. Pseudocolor images of total (YFP) and internalized BACE1 (BTX fluorescence) in representative neurons among the set of neurons used for quantitative analysis is shown. Insets show magnified segments of axons.

(B) Mean axon and dendrite fluorescence intensities for total (YFP) and internalized BACE1 (BTX fluorescence) were quantified from individual neurons (n = 11–15 neurons each) and used to calculate axon:dendrite ratios. Note the significant decrease of axonal BACE1 localization in neurons expressing EHD-ΔEH.

(C) Quantification of BACE1-YFP vesicle motility in axons of neurons cotransfected with the indicated construct. vector n = 773, EHD1 WT n = 412, EHD1-ΔEH n = 385, EHD3 WT n = 952, EHD3-ΔEH n = 281 vesicles were analyzed from 7–14 neurons.

(D) Representative kymograph analysis of BACE1-YFP transport in axons of transfected neurons is shown.

(E) Neurons were cotransfected with NPY-mCherry and empty vector or the indicated GFP-tagged EHD-ΔEH constructs. Representative kymographs of NPY-mCherry axonal transport are shown.

Error bars represent SEM. See also Figure S5.

accompanied by a concomitant decrease in the levels of total and internalized BACE1 in axons, raising the intriguing possibility that internalized BACE1 in dendrites reaches the soma and is ultimately targeted to axons by transcytotic transport. Our characterization of a role for EHD proteins in BACE1 sorting and axonal transport is highly relevant to physiological Aβ production because of the compelling in vivo data on axonal transport and BACE1 processing of APP during transit and the release of Aβ near presynaptic sites (Buxbaum et al., 1998; Lazarov et al., 2002; Sheng et al., 2002; Cirrito et al., 2005; Harris et al., 2010; Sokolow et al., 2012). Based on the identification of several neuronal membrane proteins as BACE1 substrates, including L1/NgCAM (Zhou et al., 2012; Kuhn et al., 2012), it is conceivable that axonal localization of BACE1 serves an important physiological role in the nervous system, in addition to its most investigated function in Aβ production.

The Pathological Relevance of Endosomal BACE1 Trafficking and Axonal Sorting

Dysfunction of endosomal protein sorting (such as accumulation of Aβ within enlarged early endosomes that contain Rab4 and Rab5) has been implicated in pathogenesis of sporadic Alzheimer's disease (reviewed in Rajendran and Annaert, 2012). It has been proposed that APP and its secretases are transported in distinct secretory and/or endosomal organelles under physiological conditions but begin to accumulate in enlarged endosomes during disease onset, increasing the chances of amyloidogenic processing, a notion that is consistent with studies that employed the $Rab5_{Q79L}$ mutant (Sannerud et al., 2011). In addition to Rab5, experimental perturbations of protein function or

alterations in the expression of several mediators of endocytic sorting, such as NEEP21, sorLA/LR11, GGA family members, retromer complex subunits, ADP-ribosylation factor 6, sorting nexin 17, and phosphatidylinositol clathrin assembly lymphoid-myeloid leukemia protein (PICALM), have been reported to affect APP processing and Aβ production. We have identified EHD1 and EHD3 as regulators of BACE1 trafficking in neurons. Knockdown of EHD expression in primary neurons significantly reduced Aβ secretion, implicating EHD function in neuronal APP processing. These findings may also have functional relevance to abnormal presynaptic accumulation of BACE1 near amyloid plaques documented in Alzheimer's disease (Zhao et al., 2007). Interestingly, Rab11 GTPase, which forms a complex with EHD proteins via Rab11FIP2, was independently identified as one of the two major regulators of Aβ production in mammalian cells in an unbiased paired RNAi screen of human Rab GTPases and Rab GTPase-activating proteins (Udayar et al., 2013). In conclusion, our studies demonstrate a role for EHD proteins in regulating unidirectional dendritic BACE1 transport and axonal sorting and provide insights into cellular mechanisms responsible for BACE1 localization and Aβ release near presynaptic sites.

EXPERIMENTAL PROCEDURES

cDNA Constructs

C-terminally EYFP-tagged BACE1 was generated by subcloning mouse BACE1 cDNA (provided by Dr. Nabil G. Seidah) in-frame into the pEYFP-N1 vector. A similar strategy was used to generate BACE1-Cerulean. A 13-amino-acid α-*B*ungaratoxin *B*inding *S*ite (BBS) (Sekine-Aizawa and Huganir, 2004) was inserted after the prodomain of BACE1, to generate BBS-BACE1-YFP. The dileucine mutation (L499A/L500A) was introduced by PCR mutagenesis. To generate mouse Rab11B, a mouse brain PCR product that codes for amino acids 72 to 218 was exchanged for the corresponding region in HA-tagged Rab11A construct (Ren et al., 1998). The cDNA inserts were then subcloned in-frame into the pmCherry-C1 vector. All constructs were verified by sequencing. DsRed-, GFP-, or myc-tagged human EHD1 and three plasmids have been described (George et al., 2007). NPY-mCherry was provided by Dr. Gary Banker.

BTX-Labeling Assay Development

HeLa cells plated on coverslips were transfected with BBS-BACE1WT-YFP using Lipofectamine 2000. For the BTX uptake experiments, cells were incubated the next day with 6.7 μg/ml AF555-BTX (Molecular Probes) at 37°C for 1 hr. Coverslips were then gently washed twice in cold Hanks' balanced salt solution with 10 mM HEPES (pH 7.3) (HBSS). BTX bound to cell-surface BACE1 was removed by incubation in an acidic solution (0.5 M NaCl and 0.2 M acetic acid [pH 2.8]) for 5 min on ice (acid wash). For surface labeling, transfected cells were incubated at 10°C for 20 min with 13.3 μg/ml AF555-BTX in complete culture medium. The coverslips were washed twice in cold HBSS, and one set of coverslips was further subjected to acid wash. Cells were fixed in 4% PFA/4% sucrose for 20 min at room temperature, and nuclei were stained with 0.25 μg/ml Hoechst 33342 (Molecular Probes) before mounting the coverslips.

HEK cells stably expressing BBS-BACE1WT-YFP were plated in a 96-well black glass-bottom plate (Costar) pretreated with poly-L-lysine (Sigma) to optimize cell adhesion. Eighteen hours after plating, cells were incubated at 37°C with 4 μg/ml AF647-BTX for a range of time points as indicated (time course experiment in Figure 1D). After the incubation, cells were gently washed three times on ice with PBS and fixed. Fluorescence intensities were quantified a Tecan Safire2 microplate reader (Tecan). Nontransfected HEK cells were assayed alongside as a control for background subtraction. Three wells were used for each time point, and the experiment was independently repeated three times. A standard curve was generated in each experiment using a range of cell densities assayed by BTX uptake for 1 hr.

Labeling of Surface and Internalized BACE1 in Neurons

All animal studies were approved by the Institutional Animal Care and Use Committee and conducted in accordance with University of Chicago Animal Care Guide lines. Hippocampal neurons were cultured from E17 mouse embryos as previously described (Kaech and Banker, 2006). Dissociated neurons were cultured on poly-D-lysine coated glass coverslips suspended over a monolayer of primary astrocytes prepared from P0–P2 mouse pups. Cultures were maintained in Neurobasal supplemented with B27 serum-free and GlutaMAX-I supplement (Invitrogen). Neurons were transfected with Lipofectamine 2000 (Invitrogen) on DIV11 and fixed for immunostaining or used for live-cell imaging between DIV12 and 14. In BTX uptake experiments AF647- or AF555-conjugated BTX (Invitrogen) was added to the culture medium (6.6 or 2 μg/ml, respectively), at 37°C for 3–4 hr. Coverslips were washed with ice-cold Hanks' balanced salt solution with 10 mM HEPES (pH 7.3) (HBSS), and BTX bound to cell-surface BACE1 was removed by a 2 min acid wash. Subsequently neurons were fixed and stained with antibodies against MAP2 and endosome markers (see Supplemental Experimental Procedures). For live-cell imaging, coverslips were washed after BTX uptake with imaging medium (119 mM NaCl, 2.5 mM KCl, 2 mM $CaCl_2$, 2 mM $MgCl_2$, 30 mM D-glucose, and 25 mM HEPES [pH 7.4]) before image acquisition. For surface staining, neurons were incubated on ice with culture medium containing 13.33 μg/ml AF647-BTX for 20 min.

Image Acquisition and Analysis

Wide-field epifluorescence images of fixed neurons were acquired as 200 nm z stacks using 20× (NA 0.75) or 60× (NA 1.49) objectives. Confocal images were acquired using a Leica SP5 II STED-CW Superresolution Laser Scanning Confocal microscope using 10× (NA 0.4) and 100× (NA 1.4; zoom 2.5) objectives. Quantitative analysis was performed using Metamorph (Molecular Devices) and ImageJ software. Additional information on image processing is detailed in the Supplemental Experimental Procedures. Axonal and dendritic BACE1 fluorescence intensities were quantified on 60× z stack projections of neurons using an established method (Sampo et al., 2003; Farías et al., 2012). Briefly, the average fluorescence intensities were measured along 100–200 μm-long one-pixel-wide line segments traced on two to three representative sections of dendrites and axons in each neuron using ImageJ. The mean fluorescence intensity in the soma was quantified by drawing a region around the soma. The average axon:dendrite ratio was calculated for each neuron. Manders' coefficient of colocalization of BACE1 with organelles markers or tagged proteins was calculated on thresholded confocal images of dendrites or 60× deconvolved z stack projections of axons (identified by MAP2 staining) using JACoP ImageJ plugin (Bolte and Cordelières, 2006).

Live-Cell Imaging

Live-cell images were acquired on a motorized Nikon TE 2000 microscope maintained at 37°C in a custom-designed environment chamber, at the rate of one frame/s, using 60× (NA 1.49) objective and Cascade II:512 CCD camera (Photometrics). Image stacks were processed in ImageJ software. Kymographs were generated in Metamorph and used to determine the frequency and directionality of movement of transport vesicles that moved at the rate of >0.1 μm/sec.

Immunohistochemistry and Immunofluorescence Staining

The antibodies and methods used for staining human and mouse brain tissue are described under Supplemental Experimental Procedures (Zhao et al., 2007; Gong et al., 2011).

siRNA Transfection in Primary Neurons and Aβ Quantification

Chemically synthesized stealth siRNAs from Invitrogen were used to knock down endogenous *EHD1* and *EHD3* expression in primary mouse neuronal cultures. A pool of four different siRNAs was transfected into DIV5 neurons

at a final concentration of 100 nM using Lipofectamine RNAiMAX (Invitrogen). The siRNA sequences used were as follows:

Sense sequences:

EHD1-oligo1, CCGCCCUCAGGAAGCUCAAUGACCU;
EHD1-oligo2, GGGCAUUGAUGAUGUUGAGUGGGUA;
EHD1-oligo3, GGAAGAUCUGGAAGUUGGCAGAUGU;
EHD1-oligo4, CAGCAUCAGCAUCAUUGACACUCCU;
EHD3-oligo1, UGGCUCAUGACAUUGCCCAGCUCAU;
EHD3-oligo2, GGUGAACAACCUGGCUGAGAUCUAU;
EHD3-oligo3, GGGUGGACCGAAUUAUCCUACUCUU;
and EHD3-oligo4, CCUUCAUCAGGUACCUGCUGGAACA.

Antisense sequences:

EHD1-oligo1, AGGUCAUUGAGCUUCCUGAGGGCGG;
EHD1-oligo2, UACCCACUCAACAUCAUCAAUGCCC;
EHD1-oligo3, ACAUCUGCCAACUUCCAGAUCUUCC;
EHD1-oligo4, AGGAGUGUCAAUGAUGCUGAUGCUG;
EHD3-oligo1, AUGAGCUGGGCAAUGUCAUGAGCCA;
EHD3-oligo2, AUAGAUCUCAGCCAGGUUGUUCACC;
EHD3-oligo3, AAGAGUAGGAUAAUUCGGUCCACCC;
and EHD3-oligo4, UGUUCCAGCAGGUACCUGAUGAAGG.

Conditioned medium was collected and assayed for Aβ essentially as described (Bali et al., 2012). An electrochemiluminescene assay was used to measure Aβ38, Aβ40, and Aβ42 in a mouse specific 96-well MULTI-ARRAY multiplex kit (Meso Scale Discovery).

Real-Time RT-PCR

Total RNA from mouse primary neurons was isolated using TRIzol (Invitrogen) and cDNA was prepared using the iScript cDNA synthesis kit (BIO-RAD) according to the manufacturer's recommended protocol. Real-time PCR was performed using iTaq Universal SYBR Green Supermix (BIO-RAD). Relative *EHD1* and *EHD3* gene expression levels were calculated with the ΔΔCt method using *GAPDH* for normalization.

Statistical Analysis

Each experiment was performed using at least three independent sets of cultures. Data are presented as mean ± SEM. Statistical significance was determined by t tests (comparison of two groups; Figures 2C, 6B, and S1C) or ANOVA (comparison of three or more groups) using GraphPad Prism software and indicated the figures: *$p < 0.05$; **$p < 0.01$; ***$p < 0.001$; ****$p < 0.0001$; ns, nonsignificant.

SUPPLEMENTAL INFORMATION

Supplemental Information includes Supplemental Experimental Procedures, five figures, and five movies and can be found with this article online at http://dx.doi.org/10.1016/j.celrep.2013.12.006.

ACKNOWLEDGMENTS

We thank Drs. Sangram, S. Sisodia, Kamal Sharma, Marie-Claude Potier, and Vladimir I. Gelfand for helpful discussions. This work was supported by grants from the National Institutes of Health (AG019070 and AG021495 to G.T.; AG022560 and AG030142 to R.V.; CA105489, CA99163, CA87986, and CA116552 to H.B.; and NS055223 to A.T.P.), Cure Alzheimer's Fund (G.T. and R.V.), BrightFocus Foundation (G.T.), and Alzheimer's Association (G.T.). L.R. was supported by the Swiss National Science Foundation, the Velux Foundation, Bangerter Stiftung, Baugarten Stiftung, and the Novartis Foundation. L.R. and V.U. were supported by the European Neuroscience Campus of the Erasmus Mundus Program. V.B.-P. was partially supported by a fellowship from Alzheimer's Disease Research Fund of Illinois Department of Public Health. C.G.F. and M.L. were supported by National Institute of General Medical Sciences training grant GM07839-30. Confocal imaging was performed at the Integrated Microscopy Core Facility at the University of Chicago (supported by S10 OD010649).

Received: July 24, 2012
Revised: November 7, 2013
Accepted: December 3, 2013
Published: December 26, 2013

REFERENCES

Baas, P.W., Deitch, J.S., Black, M.M., and Banker, G.A. (1988). Polarity orientation of microtubules in hippocampal neurons: uniformity in the axon and nonuniformity in the dendrite. Proc. Natl. Acad. Sci. USA *85*, 8335–8339.

Bali, J., Gheinani, A.H., Zurbriggen, S., and Rajendran, L. (2012). Role of genes linked to sporadic Alzheimer's disease risk in the production of β-amyloid peptides. Proc. Natl. Acad. Sci. USA *109*, 15307–15311.

Bel, C., Oguievetskaia, K., Pitaval, C., Goutebroze, L., and Faivre-Sarrailh, C. (2009). Axonal targeting of Caspr2 in hippocampal neurons via selective somatodendritic endocytosis. J. Cell Sci. *122*, 3403–3413.

Bolte, S., and Cordelières, F.P. (2006). A guided tour into subcellular colocalization analysis in light microscopy. J. Microsc. *224*, 213–232.

Burack, M.A., Silverman, M.A., and Banker, G. (2000). The role of selective transport in neuronal protein sorting. Neuron *26*, 465–472.

Buxbaum, J.D., Thinakaran, G., Koliatsos, V., O'Callahan, J., Slunt, H.H., Price, D.L., and Sisodia, S.S. (1998). Alzheimer amyloid protein precursor in the rat hippocampus: transport and processing through the perforant path. J. Neurosci. *18*, 9629–9637.

Chia, P.Z., Toh, W.H., Sharples, R., Gasnereau, I., Hill, A.F., and Gleeson, P.A. (2013). Intracellular itinerary of internalised β-secretase, BACE1, and its potential impact on β-amyloid peptide biogenesis. Traffic *14*, 997–1013.

Cirrito, J.R., Yamada, K.A., Finn, M.B., Sloviter, R.S., Bales, K.R., May, P.C., Schoepp, D.D., Paul, S.M., Mennerick, S., and Holtzman, D.M. (2005). Synaptic activity regulates interstitial fluid amyloid-beta levels in vivo. Neuron *48*, 913–922.

Cirrito, J.R., Kang, J.E., Lee, J., Stewart, F.R., Verges, D.K., Silverio, L.M., Bu, G., Mennerick, S., and Holtzman, D.M. (2008). Endocytosis is required for synaptic activity-dependent release of amyloid-beta in vivo. Neuron *58*, 42–51.

Das, U., Scott, D.A., Ganguly, A., Koo, E.H., Tang, Y., and Roy, S. (2013). Activity-induced convergence of APP and BACE-1 in acidic microdomains via an endocytosis-dependent pathway. Neuron *79*, 447–460.

Farías, G.G., Cuitino, L., Guo, X., Ren, X., Jarnik, M., Mattera, R., and Bonifacino, J.S. (2012). Signal-mediated, AP-1/clathrin-dependent sorting of transmembrane receptors to the somatodendritic domain of hippocampal neurons. Neuron *75*, 810–823.

George, M., Ying, G., Rainey, M.A., Solomon, A., Parikh, P.T., Gao, Q., Band, V., and Band, H. (2007). Shared as well as distinct roles of EHD proteins revealed by biochemical and functional comparisons in mammalian cells and C. elegans. BMC Cell Biol. *8*, 3.

Goldsbury, C., Mocanu, M.M., Thies, E., Kaether, C., Haass, C., Keller, P., Biernat, J., Mandelkow, E., and Mandelkow, E.M. (2006). Inhibition of APP trafficking by tau protein does not increase the generation of amyloid-beta peptides. Traffic *7*, 873–888.

Gong, P., Roseman, J., Fernandez, C.G., Vetrivel, K.S., Bindokas, V.P., Zitzow, L.A., Kar, S., Parent, A.T., and Thinakaran, G. (2011). Transgenic neuronal overexpression reveals that stringently regulated p23 expression is critical for coordinated movement in mice. Mol. Neurodegener. *6*, 87.

Haass, C., Kaether, C., Thinakaran, G., and Sisoda, S.S. (2012). Trafficking and proteolytic processing of APP. In The Biology of Alzheimer disease, D.J. Selkoe, E. Mandelkow, and D.M. Holtzman, eds. (Cold Spring Harbor: Cold Spring Harbor Laboratory Press), pp. 205–229.

Harris, J.A., Devidze, N., Verret, L., Ho, K., Halabisky, B., Thwin, M.T., Kim, D., Hamto, P., Lo, I., Yu, G.Q., et al. (2010). Transsynaptic progression of amyloid-β-induced neuronal dysfunction within the entorhinal-hippocampal network. Neuron *68*, 428–441.

He, X., Chang, W.P., Koelsch, G., and Tang, J. (2002). Memapsin 2 (beta-secretase) cytosolic domain binds to the VHS domains of GGA1 and

GGA2: implications on the endocytosis mechanism of memapsin 2. FEBS Lett. *524*, 183–187.

Huse, J.T., Pijak, D.S., Leslie, G.J., Lee, V.M., and Doms, R.W. (2000). Maturation and endosomal targeting of beta-site amyloid precursor protein-cleaving enzyme. The Alzheimer's disease beta-secretase. J. Biol. Chem. *275*, 33729–33737.

Jonsson, T., Atwal, J.K., Steinberg, S., Snaedal, J., Jonsson, P.V., Bjornsson, S., Stefansson, H., Sulem, P., Gudbjartsson, D., Maloney, J., et al. (2012). A mutation in APP protects against Alzheimer's disease and age-related cognitive decline. Nature *488*, 96–99.

Kaech, S., and Banker, G. (2006). Culturing hippocampal neurons. Nat. Protoc. *1*, 2406–2415.

Kuhn, P.H., Koroniak, K., Hogl, S., Colombo, A., Zeitschel, U., Willem, M., Volbracht, C., Schepers, U., Imhof, A., Hoffmeister, A., et al. (2012). Secretome protein enrichment identifies physiological BACE1 protease substrates in neurons. EMBO J. *31*, 3157–3168.

Laird, F.M., Cai, H., Savonenko, A.V., Farah, M.H., He, K., Melnikova, T., Wen, H., Chiang, H.C., Xu, G., Koliatsos, V.E., et al. (2005). BACE1, a major determinant of selective vulnerability of the brain to amyloid-beta amyloidogenesis, is essential for cognitive, emotional, and synaptic functions. J. Neurosci. *25*, 11693–11709.

Lasiecka, Z.M., and Winckler, B. (2011). Mechanisms of polarized membrane trafficking in neurons — focusing in on endosomes. Mol. Cell. Neurosci. *48*, 278–287.

Lasiecka, Z.M., Yap, C.C., Caplan, S., and Winckler, B. (2010). Neuronal early endosomes require EHD1 for L1/NgCAM trafficking. J. Neurosci. *30*, 16485–16497.

Lazarov, O., Lee, M., Peterson, D.A., and Sisodia, S.S. (2002). Evidence that synaptically released beta-amyloid accumulates as extracellular deposits in the hippocampus of transgenic mice. J. Neurosci. *22*, 9785–9793.

Naslavsky, N., and Caplan, S. (2011). EHD proteins: key conductors of endocytic transport. Trends Cell Biol. *21*, 122–131.

Prabhu, Y., Burgos, P.V., Schindler, C., Farías, G.G., Magadán, J.G., and Bonifacino, J.S. (2012). Adaptor protein 2-mediated endocytosis of the β-secretase BACE1 is dispensable for amyloid precursor protein processing. Mol. Biol. Cell *23*, 2339–2351.

Prekeris, R., Foletti, D.L., and Scheller, R.H. (1999). Dynamics of tubulovesicular recycling endosomes in hippocampal neurons. J. Neurosci. *19*, 10324–10337.

Rajendran, L., and Annaert, W. (2012). Membrane trafficking pathways in Alzheimer's disease. Traffic *13*, 759–770.

Ren, M., Xu, G., Zeng, J., De Lemos-Chiarandini, C., Adesnik, M., and Sabatini, D.D. (1998). Hydrolysis of GTP on rab11 is required for the direct delivery of transferrin from the pericentriolar recycling compartment to the cell surface but not from sorting endosomes. Proc. Natl. Acad. Sci. USA *95*, 6187–6192.

Sampo, B., Kaech, S., Kunz, S., and Banker, G. (2003). Two distinct mechanisms target membrane proteins to the axonal surface. Neuron *37*, 611–624.

Sannerud, R., Declerck, I., Peric, A., Raemaekers, T., Menendez, G., Zhou, L., Veerle, B., Coen, K., Munck, S., De Strooper, B., et al. (2011). ADP ribosylation factor 6 (ARF6) controls amyloid precursor protein (APP) processing by mediating the endosomal sorting of BACE1. Proc. Natl. Acad. Sci. USA *108*, E559–E568.

Sekine-Aizawa, Y., and Huganir, R.L. (2004). Imaging of receptor trafficking by using alpha-bungarotoxin-binding-site-tagged receptors. Proc. Natl. Acad. Sci. USA *101*, 17114–17119.

Sheng, J.G., Price, D.L., and Koliatsos, V.E. (2002). Disruption of corticocortical connections ameliorates amyloid burden in terminal fields in a transgenic model of Abeta amyloidosis. J. Neurosci. *22*, 9794–9799.

Sokolow, S., Luu, S.H., Nandy, K., Miller, C.A., Vinters, H.V., Poon, W.W., and Gylys, K.H. (2012). Preferential accumulation of amyloid-beta in presynaptic glutamatergic terminals (VGluT1 and VGluT2) in Alzheimer's disease cortex. Neurobiol. Dis. *45*, 381–387.

Sönnichsen, B., De Renzis, S., Nielsen, E., Rietdorf, J., and Zerial, M. (2000). Distinct membrane domains on endosomes in the recycling pathway visualized by multicolor imaging of Rab4, Rab5, and Rab11. J. Cell Biol. *149*, 901–914.

Thinakaran, G., and Koo, E.H. (2008). Amyloid precursor protein trafficking, processing, and function. J. Biol. Chem. *283*, 29615–29619.

Udayar, V., Buggia-Prevot, V., Guerreiro, R.L., Siegel, G., Rambabu, N., Soohoo, A.L., Ponnuswamy, M., Siegenthaler, B., Bali, J., et al.; AESG (2013). A paired RNAi and RabGAP overexpression screen identifies Rab11 as a regulator of β-amyloid production. Cell Rep. *5*, this issue, 1536–1551.

Vassar, R., Bennett, B.D., Babu-Khan, S., Kahn, S., Mendiaz, E.A., Denis, P., Teplow, D.B., Ross, S., Amarante, P., Loeloff, R., et al. (1999). Beta-secretase cleavage of Alzheimer's amyloid precursor protein by the transmembrane aspartic protease BACE. Science *286*, 735–741.

Yan, R., Bienkowski, M.J., Shuck, M.E., Miao, H., Tory, M.C., Pauley, A.M., Brashier, J.R., Stratman, N.C., Mathews, W.R., Buhl, A.E., et al. (1999). Membrane-anchored aspartyl protease with Alzheimer's disease beta-secretase activity. Nature *402*, 533–537.

Yap, C.C., and Winckler, B. (2012). Harnessing the power of the endosome to regulate neural development. Neuron *74*, 440–451.

Yap, C.C., Wisco, D., Kujala, P., Lasiecka, Z.M., Cannon, J.T., Chang, M.C., Hirling, H., Klumperman, J., and Winckler, B. (2008). The somatodendritic endosomal regulator NEEP21 facilitates axonal targeting of L1/NgCAM. J. Cell Biol. *180*, 827–842.

Yap, C.C., Lasiecka, Z.M., Caplan, S., and Winckler, B. (2010). Alterations of EHD1/EHD4 protein levels interfere with L1/NgCAM endocytosis in neurons and disrupt axonal targeting. J. Neurosci. *30*, 6646–6657.

Zhao, J., Fu, Y., Yasvoina, M., Shao, P., Hitt, B., O'Connor, T., Logan, S., Maus, E., Citron, M., Berry, R., et al. (2007). Beta-site amyloid precursor protein cleaving enzyme 1 levels become elevated in neurons around amyloid plaques: implications for Alzheimer's disease pathogenesis. J. Neurosci. *27*, 3639–3649.

Zhou, L., Barão, S., Laga, M., Bockstael, K., Borgers, M., Gijsen, H., Annaert, W., Moechars, D., Mercken, M., Gevaert, K., and De Strooper, B. (2012). The neural cell adhesion molecules L1 and CHL1 are cleaved by BACE1 protease in vivo. J. Biol. Chem. *287*, 25927–25940.